Tape casting process for fabrication of electrolyte supported solid oxide fuel cell

T. L. Gilbile[1*], Dhanjay Khankal[2] A.P. Pandhare[1].

1. Dept. of Mechanical Engg., Sinhgad college of Engineering, Vadgaon (Bk), Pune, India-41

2. Dept. of Production Engg. Sinhgad college of Engineering, Vadgaon (Bk), Pune, India-41

*Corresponding Author: tlgilbile.scoe@sinhgad.edu

Abstract

The solid oxide fuel cells (SOFC's) utilize oxidation of hydrogen fuel for generation of electricity at high temperatures. Hydrogen is used as fuel because of its high energy density. The SOFC's are studied widely because they are having high efficiency and low cost. The SOFC's can be plane or tubular geometries. However, the plane geometry SOFC provides high current density of 0.50 to 1.5 W/cm^2 compared to tubular geometry. Here the research is focused on tape casting method because of its simplicity and low manufacturing cost. A simple electrolyte supported SOFC is prepared with de-airing technique. The electrical conductivity of the electrolyte is measured with the help of electron microscopy method.

Keywords: *Tape casting, green tape, SOFC, doctors blade*

Introduction

With the major over growing concern of the availability of the fossil fuels because of its depletion at higher rate and its adverse environmental pollution has driven attention of researchers towards renewable energy sources and green energy conversion[1–4]. Thus there is an urgent need to use renewable and green energy conversion[4,5]. Various modern renewable energy sources like wind, solar, biodiesel etc., are available, but some of them are having problem of energy storage due to its generation time and consumption time gap[6]. Fuel cells are catching attraction because of very high efficient energy conversion technology and high efficiency that causes less environmental emissions. However electrical devices which converts chemical energy from fuel to electrical energy can be used as alternative fuel[7]. The SOFC's are having very high energy conversion efficiencies[8–12], can use any type of fuel for electrolysis and are flexible in design[10,13]. The high cost of SOFC's and lack of material suitability at high temperature hinder the application[6] Hence, there is need for research to decrease production cost per unit of fuel cell [14].

Various methods are available for the fabrication[15,16] of SOFC's are listed in following figure, but depending on the manufacturing cost only few of them are considered[17,18].

Fig.1.1: Types of catalyst coating method

The ionic conductivity of an electrolyte affects the performance of SOFC [19]. The LSGM is having high ionic conductivity as compared to other materials YSZ, GDC and SDC [20]. However, the performance goes on degrading when reacted with electrode at high temperatures. Hence advanced and simple manufacturing technique is to be used for producing electrolyte. The tape casting[21] is the process which is simple and a wide variety of highly porous microstructures can be produced[18,22]. The first step in tape casting process is slurry preparation.

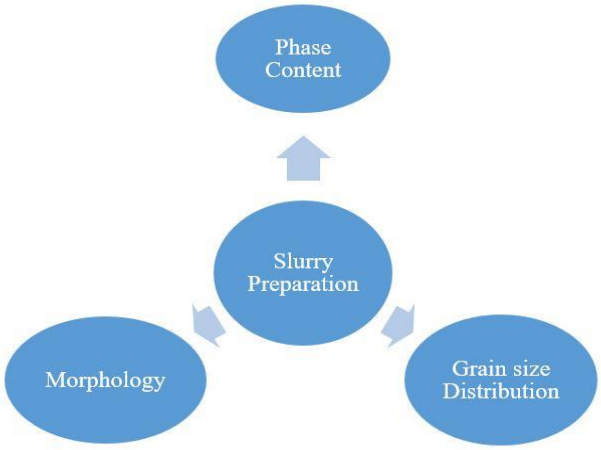

Fig.1.2: Factors affecting slurry preparation

Basic step required to be followed while preparing the slurry that is mixing of ceramic powder in solvents then milling on the machine. The role of the solvent in making the ceramic film is to increase the degree of flow ability, formability and to create a medium to carry the ceramic powder under the doctor's blade and to have the uniform distribution of ceramic powder on the substrate. Then, in that slurry (ceramic powder mixed with solvent) binders and additives (dispersants and plasticizers) are added, function of the dispersant is to get the desired properties to the ceramic power that is to increase the surface charge or lower the surface charge, high/low the surface energy or some specific surface chemistry. Plasticizers also called as sintering agent are added to increase the mechanical properties of the green tape i.e. flexibility and plasticity along with that to control the physical properties like density and microstructure with heating kinetics. Some percentage of binders is added in the ceramic powder to simply have chemical network between the ceramic powders. Average particle size and distribution of the powder i.e. is characterization of slurry is performed by the laser scattering method. Then this ceramic slurry homogenized in mixer or grinder again. Then that slurry is pumped in the reservoir in front of the doctor blade.

The slurry mixed with catalyst is poured in front of the blade. The constant force is applied on the blade then the slurry poured in front of blade spreads and a thin film is formed. The speed of the blade can be varied as per the requirement.

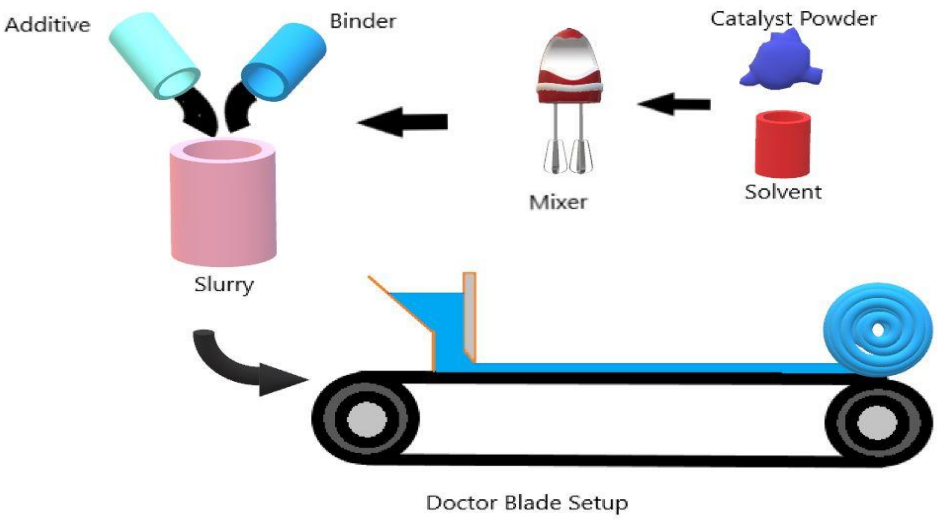

Fig.1.3: Catalyst coating process using Doctors blade

The principle of blade is depicted in figure 1.4

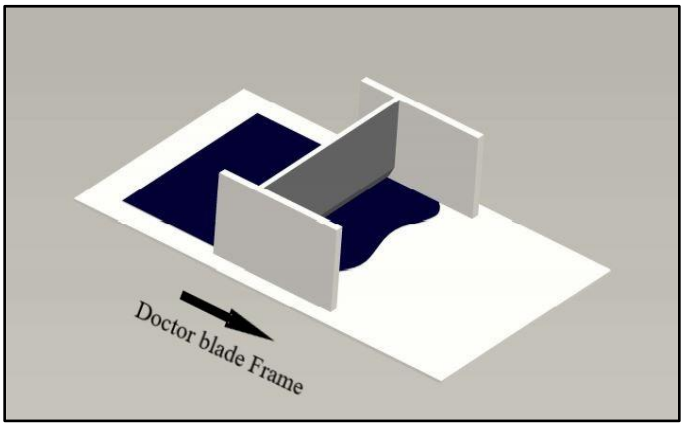

Fig.1.4: Working of doctor blade

The blade can be moved up and down depending on the thickness of the film required as shown in fig 1.5.

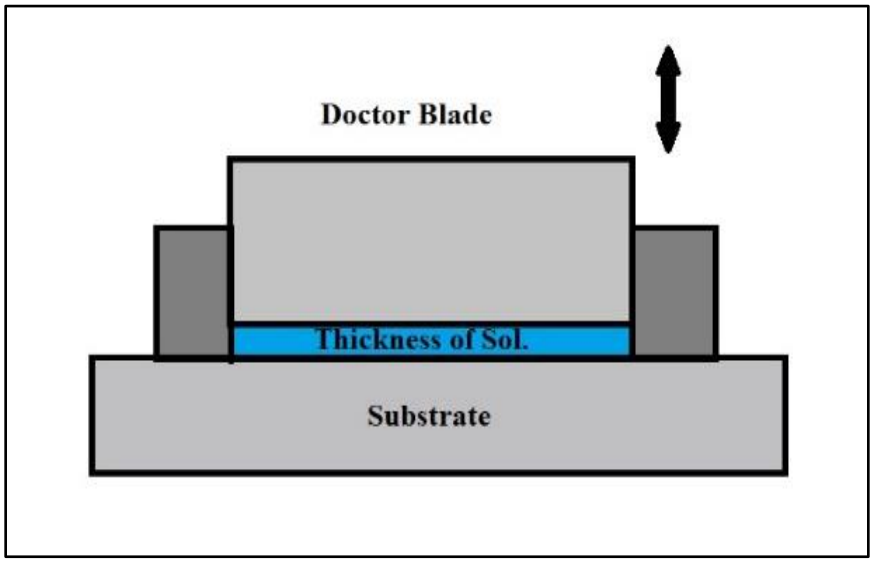

Fig. 1.5: Process of film thickness control

The precision holders are adjusted to vary the film thickness from 1-1.5mm. During the complete process of film formation, the precaution is taken that the tank remains filled with the slurry to avoid formation of bubbles. The procedure is as shown in fig 1.6.

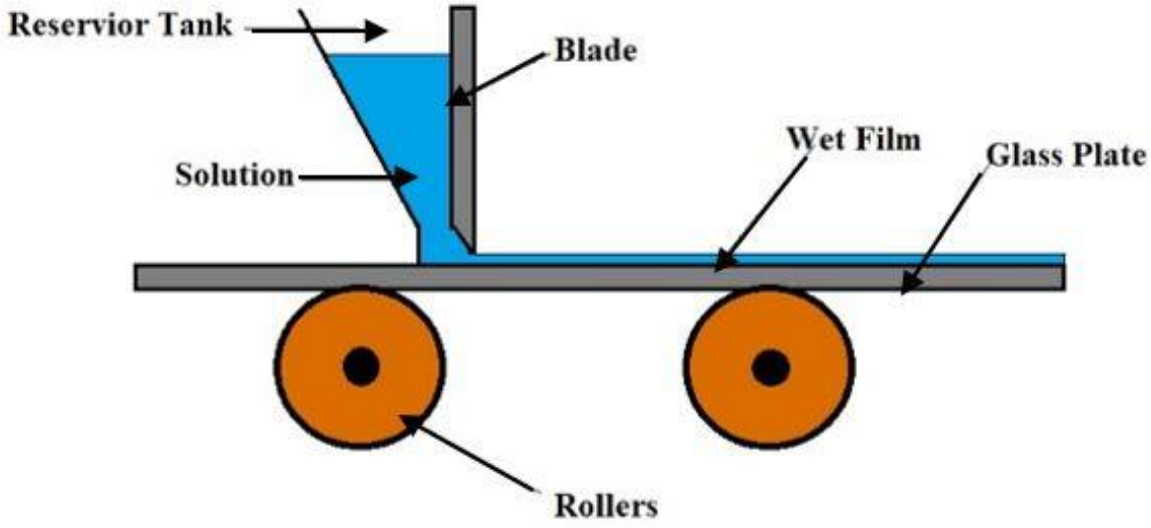

Fig.1.6: Doctor Blade coating technique for plastic foil

The viscosity plays an important role in the slurry preparation. Excessive viscosity results in poor performance tape, formation of air bubble and consequently leads to defective tape. However poor viscosity results to non-formation of the tape. The process of tape casting is shown in following flowchart (figure1.7).

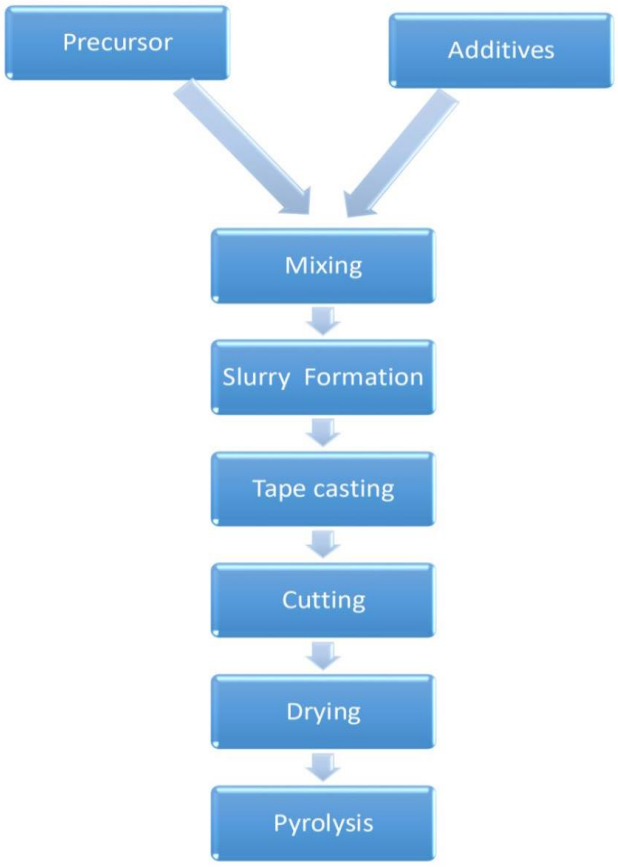

Fig.1.7: Flowchart for Tape casting process

Design of Doctors blade:

The objective of this model is to lay the membrane of thickness varying from 0.5 mm to 2.5 cm. To achieve this, the glass plate (320*600*5mm) is used as a base plate on which the catalyst membrane (300*500 mm) is to be laid using Doctors blade assembly.

The assembly consist of Doctor blade with thickness 3mm and height 40 mm supported by side support having notch of 3 mm at the both ends of the blade. To adjust the thickness of the layer required, two micrometer screw gauges are attached to one end of doctor's blade having least count 0.01mm.

In order to obtain linear movement of the doctor blade assembly, two square threaded lead screws having length of 660 mm and outer diameter of 10 mm are used. The lead screw is attached to the assembly with the help of square threaded nut having pitch 2 mm. At the end of one screw, motor is attached and at another end pulley is used. The internal diameter of the pulley is 54mm and the external diameter is 60 mm. The motion is transformed from one lead screw to another lead screw with the help pulley and toothed belt. Centre distance between two pulleys is 340 mm and length of the belt is 870 mm.

The layer created using blade needs to get cool at room temperature. Considering this requirement, 400mm*700mm air tight and dustproof compartment is designed. This compartment consists of telescopic channel slider with platform to keep the glass plate along with catalyst membrane to soke it under room temperature.

To have errorless working of the model, four height adjustment screws are provided at the four corners of the model along with level indicator.

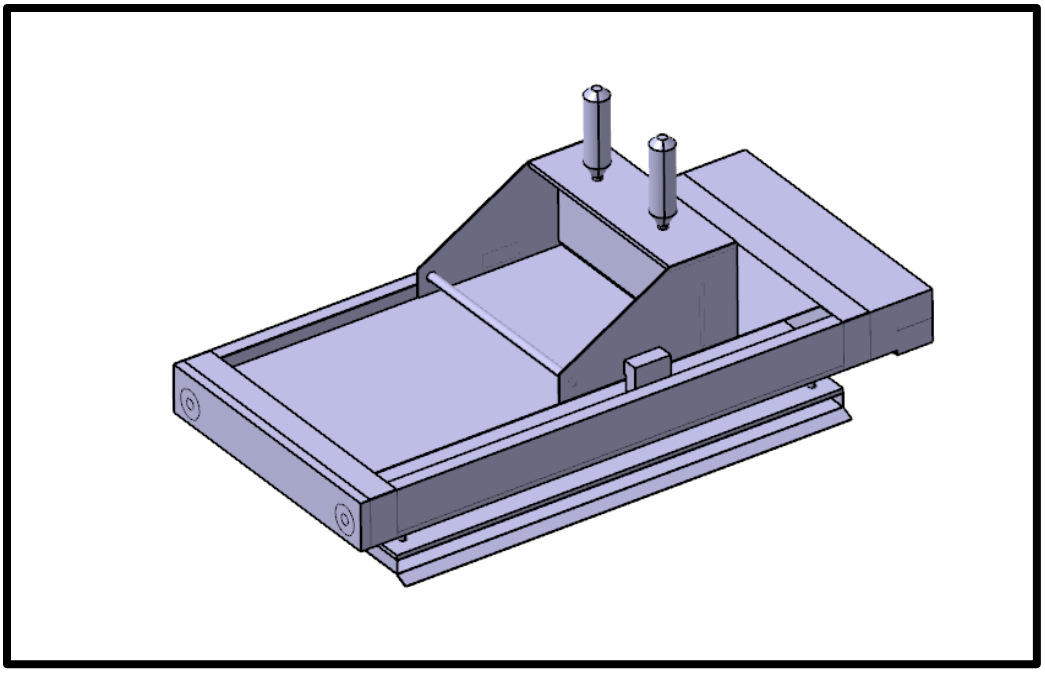

Fig.1.8: 3D cad model of doctor's blade method

CALCULATION: Component Selection for Tape casting

1. Lead screw:

Data:

Major Diameter of lead screw, D=20 mm

Minor diameter of Lead screw, d_1 = 18 mm

Efficiency of lead screw=42%

Calculation

Lead =2mm

Torque = 6.55 N-mm

Torque required to move the upper unit is 6.55 N-mm.

2. Diameter and RPM of each pulley

$d_1 * n_1 = d_2 * n_2$

d_1=60mm, n_1=20rpm

d_2=60mm, n_2=20 rpm

3. Velocity of belt

The velocity of the belt is given by

$v = \pi * d_1 * n_1 / 60$

= 0.0628 m/s

4. Length of Belt

It is given by formula

$$L = (d_1 + d_2) * \pi / 2 + 2*D + (d_1 - d_2)^2 / 4*D$$

Where D=340mm

L = 868.4=870 mm

5. **Belt tension**

We know that,

F= P/ V

F= 2.5/ 0.0628

F= 40 N

$T=P/\omega$

T= 2.5/ (2 * 3.14* 20/60)

= 1.19 Nm

ANALYSIS OF DOCTOR BLADE:

Doctor blade of 304 mm in length, 40 mm in height and thickness of blade varying from 1mm to 5 mm is considered to calculate total deformation, directional deformation and equivalent stress. At the one edge of the blade along the length, chamfer which is equal to half of the thickness has given which is shown in Fig.1.9

The static structural analysis of doctor blade (Material-HSS) is done by applying fixed support at one end as shown in fig 1.10 and force of 3N on the chamfer exerted by the slurry in the direction opposite to the direction of motion of blade as shown in fig 1.11. Here slurry viscosity is considered that of 250 grams of honey that is 10,000cP (10 Pa*s)

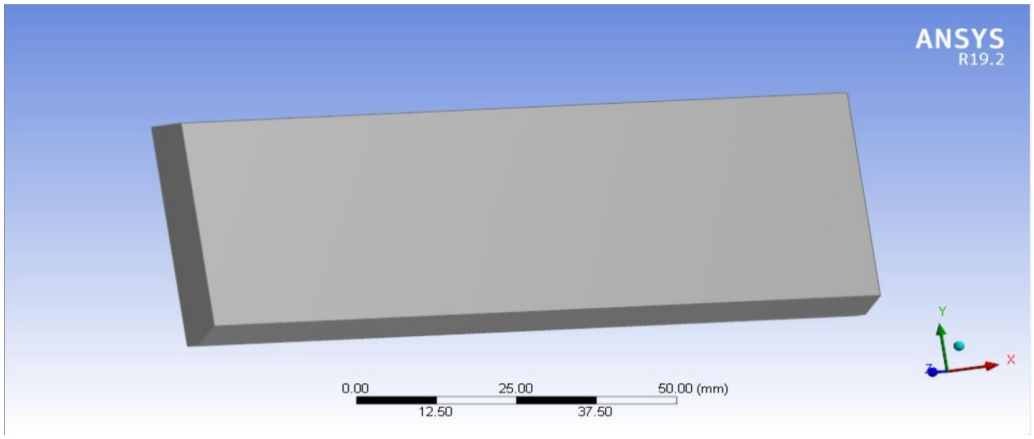

Fig.1.9: Geometry of Blade.

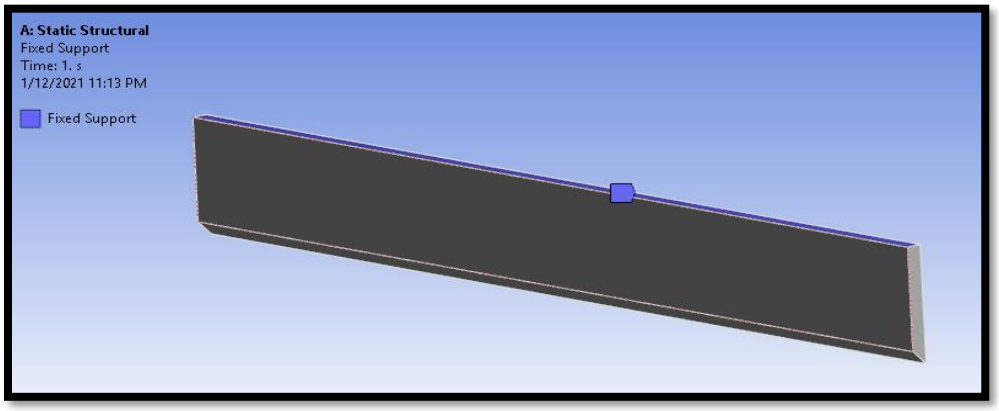

Fig.1.10: Fixed Support

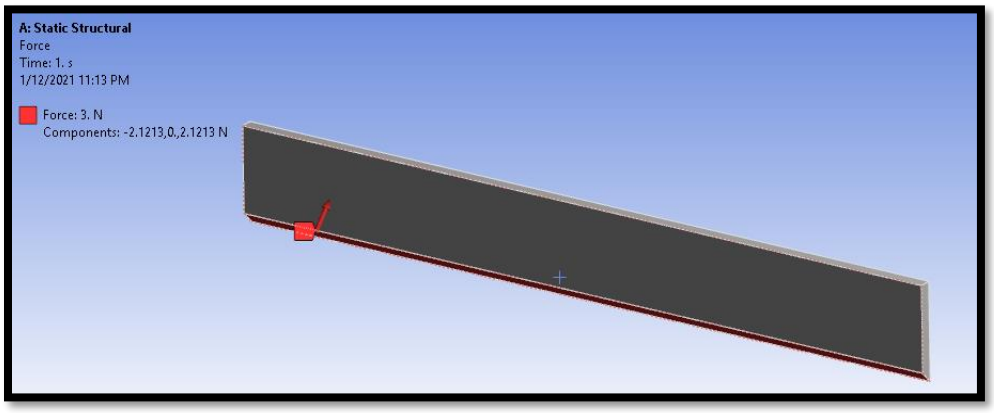

Fig.1.11: Force of 3N on the chamfer of blade

For the analysis of blade, meshing of blade is done by varying the mesh size from 0.5 to 2 mm, with step size of 0.5 mm. By varying the mesh size, total and directional deformation (mm) and Equivalent stress (MPa) is calculated which is shown in Table 3.1

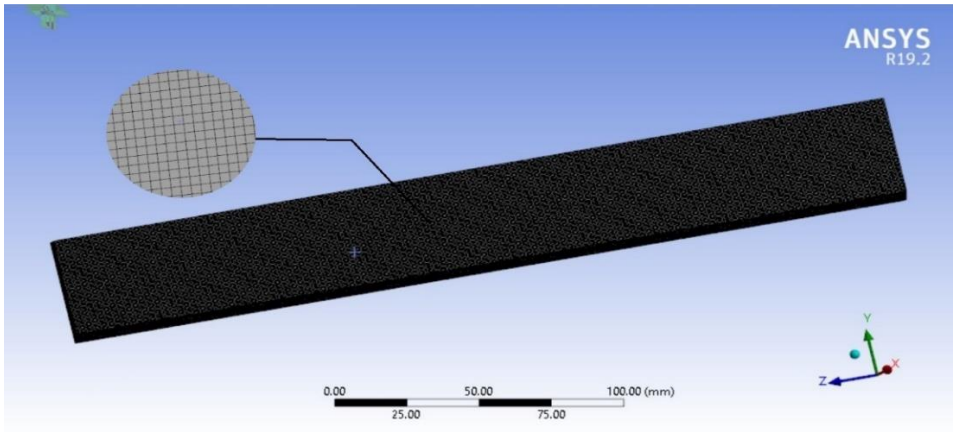

Fig.1.12: 0.5 mm Mesh on Doctor blade

Table 3.1 Values of Deformation and stress by varying mesh size

MESH SIZE (mm)	DEFORMATION (mm)		EQ. STRESS (MPa)
	TOTAL	DIRECTIONAL	
0.5	6.0731e-5	1.0263e-7	0.070055
1.0	6.0698e-5	1.0132e-7	0.059621
1.5	6.0672e-5	1.0062e-7	0.058977
2.0	6.0630e-5	0.9706e-7	0.058797

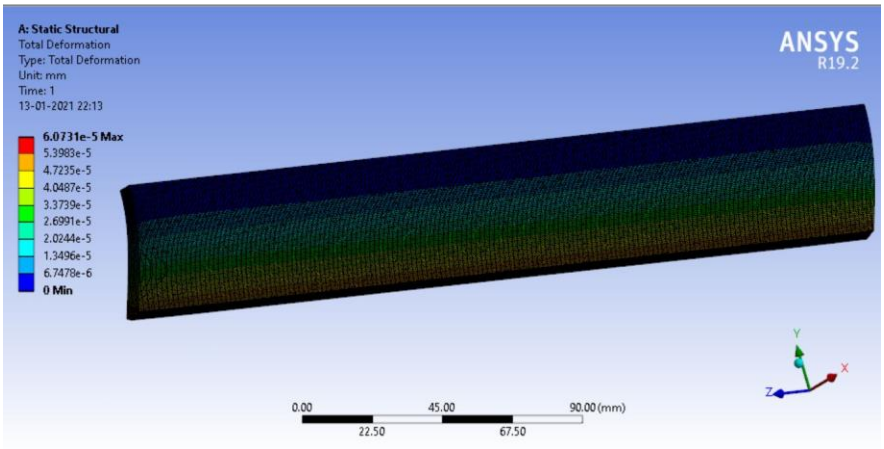

Fig.1.13: Total Deformation blade of 0.5 mm mesh size

In order to do analysis of the blade, thickness of blade is varied from 1mm to 5mm, keeping mesh size constant of 1mm. By varying the thickness of blade, total deformation (mm), Directional Deformation (mm), Equivalent stress (MPa) is calculated which is shown in Table 3.2

Table3.2 Values of Deformation and stress by varying thickness of blade

THICKNESS OF BLADE (mm)	**TOTAL DEFORMATION (mm)**	**DIRECTIONAL DEFORMATION (mm)**	**EQUIVALENT STRESS (MPa)**
1	8.0641e-3	1.0496e-6	1.6436
2	9.9238e-4	4.3314e-7	0.3936
3	2.8932e-4	2.4689e-7	0.17117
4	1.2021e-4	1.53e-7	0.0943
5	6.0687e-5	1.0148e-7	0.059511

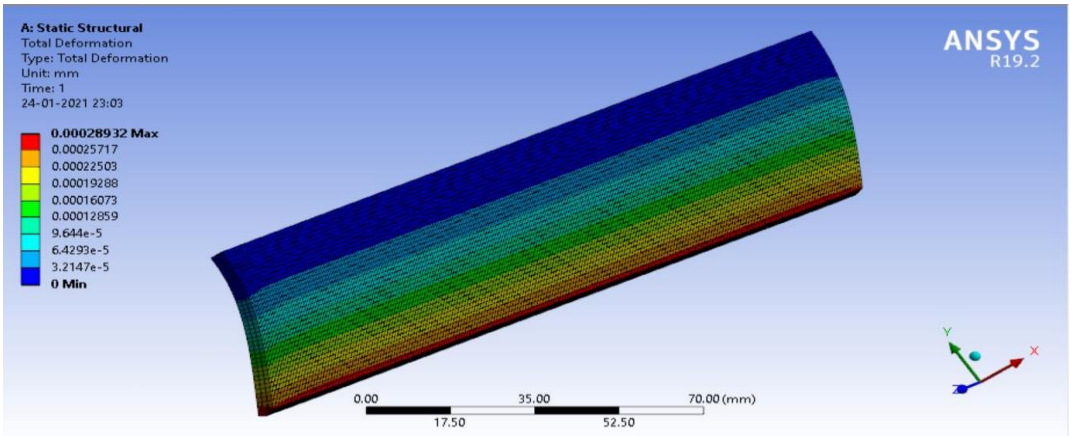

Fig.1.14: Total Deformation (mm) of blade having thickness 3 mm

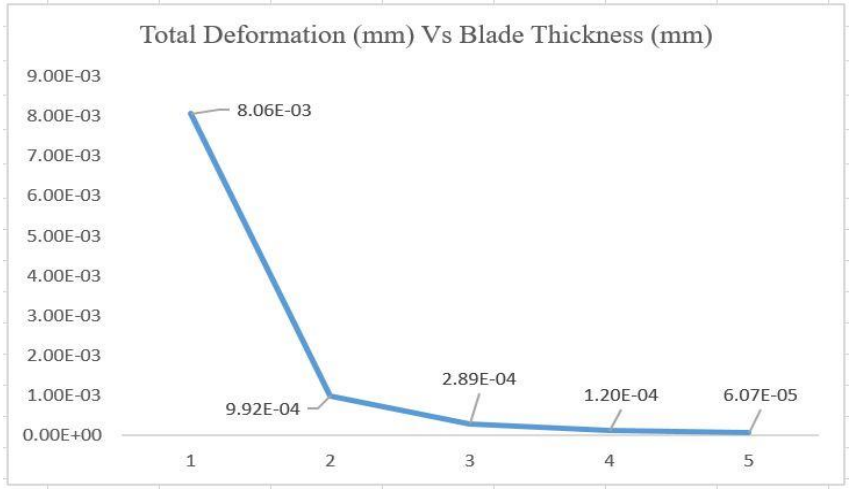

Fig.1.15 Graph of Total deformation (mm) Vs Blade Thickness (mm)

Total deformation is the vector sum of all directional displacement of the system. The graph of total deformation (mm) Vs blade thickness (mm) is shown in fig 1.14. Blade Thickness on X-axis is varied with the scale of 1 mm and total deformation with the scale of 0.001 mm on Y – axis. From this graph 1.15, it is clearly seen that total deformation goes on decreasing gradually along with increase in thickness of blade. It means that total deformation inversely varies with the blade thickness. But from blade having thickness 3 mm to 5 mm, there is no major difference in total deformation.

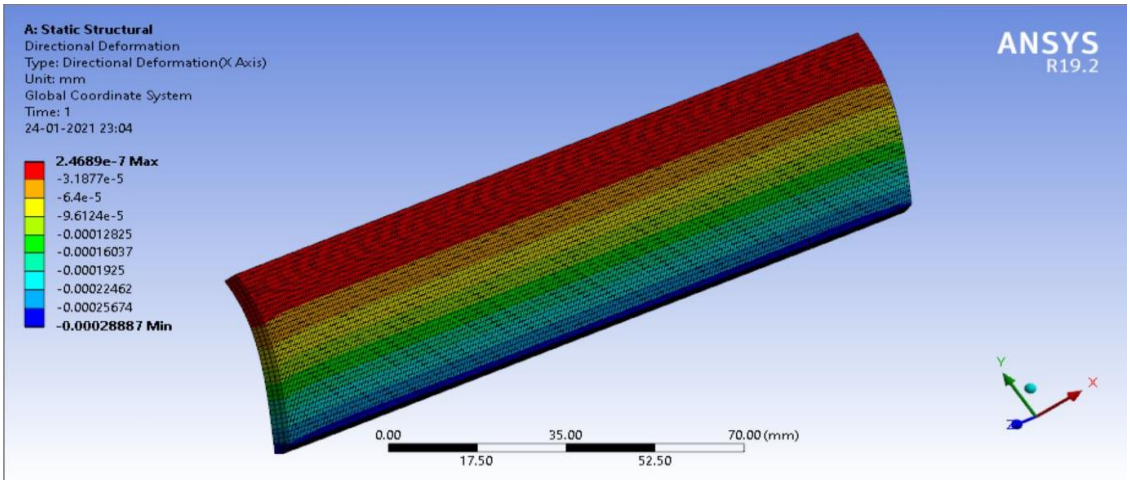

Fig.1.16: Directional Deformation blade having thickness 3mm

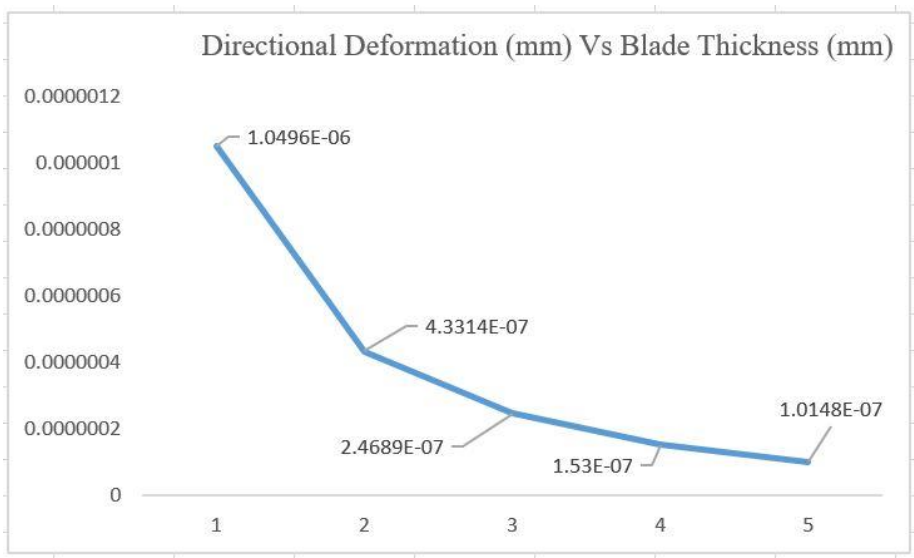

Fig.1.17 Graph of Directional Deformation (mm) Vs Blade Thickness

Directional deformation is displacement of the system in particular axis or user defined axis as shown in fig.1.16. From the graph 1.17, it is clear that, directional deformation decreases rapidly from 1mm to 3mm. But from 3mm, there is no major decreases in directional deformation Noticeable tilt is observed at blade thickness of 2 mm. Greater deformation is observed between blade thickness 1 mm to 2 mm and further up to 5 mm, slope of the curve is less.

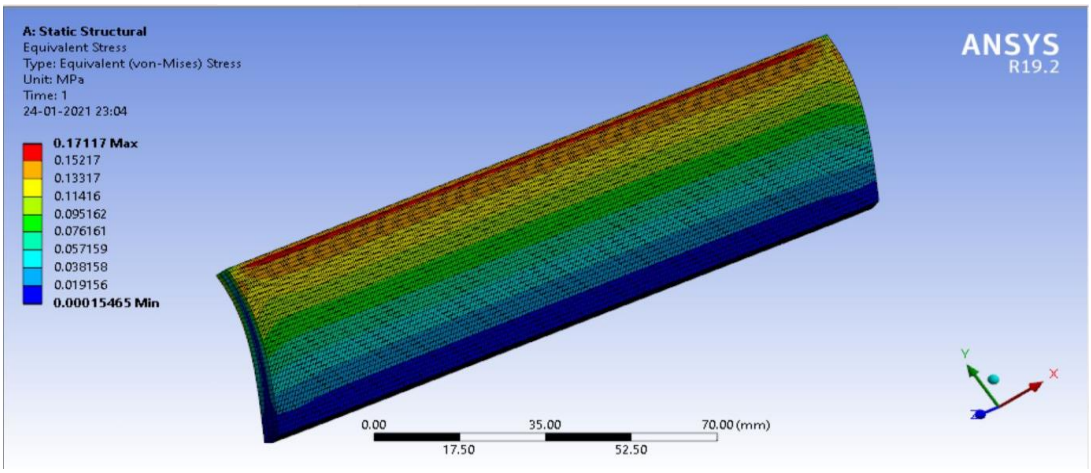

Fig.1.18: Equivalent (Von-Mises) stress on blade having thickness 3 mm

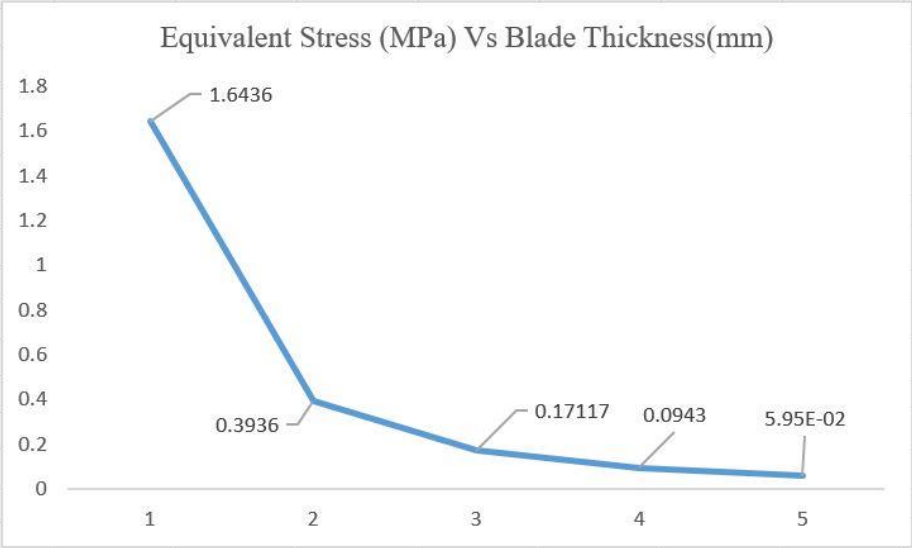

Fig.1.19: Graph of Equivalent Stress (MPa) Vs Blade Thickness (mm)

Equivalent stresses consist of effects from multiple residual stress such as principle normal stresses, principle shear stresses, energy distortion as shown in fig 1.18. The graph between equivalent stress (MPa) Vs blade thickness varying from 1 mm to 5mm is shown in fig 1.19. The graph shows negligible slope of line between blade thickness from 3 mm to 5 mm as compare to increase in the slope with blade thickness varying from 1 mm to 2 mm.
Hence the blade of thickness 3mm can be used.

CONCLUSIONS

From the drawing and analyzing the blades, following conclusion are drawn
1. The design and fabrication of the tape casting machine is successful.
2. Analysis in the ANSYS software by varying the thickness and keeping mesh size constant, best suitable thickness for the practical application with economy is 3 mm.
3. Green tapes of fuel cell (cathode, Anode, Electrolyte) with thickness variation of 20μm to 2mm are produced.
4. Maximum stress that can come and deflection of 3 mm plate by considering honey as viscous fluid are 0.17117 MPa and 2.8932 x 10^{-4} mm which are negligible that will not affect the thickness of film.
Thus, machine constructed is successful and economical for the industrial applications.

REFERENCES

[1] Kan WH, Samson AJ, Thangadurai V. Trends in electrode development for next generation solid oxide fuel cells. J Mater Chem A 2016;4:17913–32. https://doi.org/10.1039/c6ta06757c.

[2] Chen H, Cong TN, Yang W, Tan C, Li Y, Ding Y. Progress in electrical energy storage system: A critical review. Prog Nat Sci 2009;19:291–312. https://doi.org/10.1016/j.pnsc.2008.07.014.

[3] Amarsingh Bhabu K, Theerthagiri J, Madhavan J, Balu T, Muralidharan G, Rajasekaran TR. Cubic fluorite phase of samarium doped cerium oxide (CeO2)0.96Sm0.04 for solid oxide fuel cell electrolyte. J Mater Sci Mater Electron 2016;27:1566–73. https://doi.org/10.1007/s10854-015-3925-z.

[4] Shi H, Su C, Ran R, Cao J, Shao Z. Electrolyte materials for intermediate-temperature solid oxide fuel cells. Prog Nat Sci Mater Int 2020:0–1. https://doi.org/10.1016/j.pnsc.2020.09.003.

[5] Chen H, Cong TN, Yang W, Tan C, Li Y, Ding Y. Progress in electrical energy storage system: A critical review. Prog Nat Sci 2009;19:291–312. https://doi.org/10.1016/j.pnsc.2008.07.014.

[6] Kwon Y, Han Y. Using a Tape Casting Process 2020:0–6.

[7] Reisert M, Aphale A, Singh P. Solid oxide electrochemical systems: Material degradation processes and novel mitigation approaches. Materials (Basel) 2018;11. https://doi.org/10.3390/ma11112169.

[8] Loureiro FJA, Yang T, Stroppa DG, Fagg DP. Pr2O2SO4-La0.6Sr0.4Co0.2Fe0.8O3-δ: A new category of composite cathode for intermediate temperature-solid oxide fuel cells. J Mater Chem A 2015;3:12636–41. https://doi.org/10.1039/c4ta06640e.

[9] Bhattacharyya D, Rengaswamy R. A Review of Solid Oxide Fuel Cell (SOFC) Dynamic Models 2009:6068–86.

[10] Stambouli AB, Traversa E. Solid oxide fuel cells (SOFCs): A review of an environmentally clean and efficient source of energy. Renew Sustain Energy Rev 2002;6:433–55. https://doi.org/10.1016/S1364-0321(02)00014-X.

[11] Gao Z, Mogni L V., Miller EC, Railsback JG, Barnett SA. A perspective on low-temperature solid oxide fuel cells. Energy Environ Sci 2016;9:1602–44. https://doi.org/10.1039/c5ee03858h.

[12] Kochetova N, Animitsa I, Medvedev D, Demin A, Tsiakaras P. Recent activity in the

development of proton-conducting oxides for high-temperature applications. RSC Adv 2016;6:73222–68. https://doi.org/10.1039/c6ra13347a.

[13] Mahato N, Banerjee A, Gupta A, Omar S, Balani K. Progress in material selection for solid oxide fuel cell technology: A review. Prog Mater Sci 2015;72:141–337. https://doi.org/10.1016/j.pmatsci.2015.01.001.

[14] Deng Y, Peng E, Shao Y, Xiao Z, Dong Q, Huang J. Scalable fabrication of efficient organolead trihalide perovskite solar cells with doctor-bladed active layers. Energy Environ Sci 2015;8:1544–50. https://doi.org/10.1039/c4ee03907f.

[15] Richards M. Solid Oxide Fuel Cell Manufacturing Overview 2011.

[16] Rashid NLRM, Samat AA, Jais AA, Somalu MR, Muchtar A, Baharuddin NA, et al. Review on zirconate-cerate-based electrolytes for proton-conducting solid oxide fuel cell. Ceram Int 2019;45:6605–15. https://doi.org/10.1016/j.ceramint.2019.01.045.

[17] Kim H, Da Rosa C, Boaro M, Vohs JM, Gorte RJ. Fabrication of highly porous yttria-stabilized zirconia by acid leaching nickel from a nickel-yttria-stabilized zirconia cermet. J Am Ceram Soc 2002;85:1473–6. https://doi.org/10.1111/j.1151-2916.2002.tb00299.x.

[18] Thorel, Alain (Materials centre M-PC. Tape Casting Ceramics for high temperature Fuel Cell applications. Ceram Mater 2010:49–69.

[19] Lee TS, Chung JN, Chen YC. Design and optimization of a combined fuel reforming and solid oxide fuel cell system with anode off-gas recycling. Energy Convers Manag 2011;52:3214–26. https://doi.org/10.1016/j.enconman.2011.05.009.

[20] Mansilla Y, Arce M, Gonzalez Oliver C, Troiani H, Serquis A. Synthesis and characterization of ZrO2 and YSZ thin films. Mater Today Proc 2019;14:92–5. https://doi.org/10.1016/j.matpr.2019.05.060.

[21] Fiori C, De Portu G. Tape Casting: a Technique for Preparing and Studying New Materials. Br Ceram Proc 1986:213–25.

[22] Sreedhar I, Agarwal B, Goyal P, Singh SA. Recent advances in material and performance aspects of solid oxide fuel cells. J Electroanal Chem 2019;848:113315. https://doi.org/10.1016/j.jelechem.2019.113315.